NUMERICAL STUDY OF THE MECHANISM OF FORMATION OF SODIUM CHLORIDE DOMES IN GEOLOGICAL STRUCTURES DEPENDING ON THE GEOMETRICAL SIZES OF AREA

T. K. AKHMEDZHANOV, A. G. TANIRBERGENOV, ABD A. S. ELMAKSOUD[*] and B. M. NURANBAEVA

Institute of Geology and Oil Gas Business after K. Turysova, Kazakh National Technical University after Name of K. I. Satpayev, Republic of Kazakhstan Almaty, KAZAKHSTAN

ABSTRACT

The term "salt" include all rock bodies composed primarily of halite (NaCl). Salt is mechanically weak and flows like a fluid, even at geologically rapid strain rates. Salt is also relatively incompressible so is less dense than most carbonates and all moderately to fully compacted siliciclastic rocks. The primary driving force for salt tectonics is differential loading, which may be induced by gravitational forces, by forced displacement of one boundary of a salt body relative to another, or by a thermal gradient. Buoyancy considered a key driver for salt tectonics, is of secondary importance in many settings. Two factors resist salt flow: strength of the overburden and boundary drag along the edges of the salt body. Salt will move only if driving forces exceed the resistance to flow.

Salt domes are diapiric structures involving the upward flow of low-density salt. The circular nature of these features is an indication of the fact that salt domes form as a result of upward flow independent of tectonic activity. The flanks of these structures provide excellent trapping mechanisms for oil and gas. For salt domes to form, thick accumulations of salt must be overlain by sediments of higher density. The exact origin of such a large quantity of salt is not fully understood; however, it is thought that some kind of closed basin of sea water that evaporates is the major mechanism involved. The salt is then buried under unconsolidated Mesozoic and Cenozoic sediments.

Key words: Salt domes, Diapiric structures, Geological structures, Velocity, Saline, Caspian basin.

INTRODUCTION

In the Earth's crust distributed salt dome geological structures. The emergence of these geological structures are by the gravitational forces, when originally lay at the tabular

---

[*]Author for correspondence; E-mail: ashraf_sobhy2001@yahoo.com

lighter salt rock climbing, were introduced in the overlying column of sedimentary rocks in the form of salt domes (gravitational instabilities)[1,2]. In natural conditions, salt-crystalline body, under a long standing load behaves like a very viscous liquid incompressible and deformed without breaking. To study the salt domes movement, typically using heterogeneous highly viscous incompressible fluid.

The emergence and growth of salt domes can be conditionally divided into two stages, linear and non-linear. On the linear stage explores the small deformation of salt; this stage sufficiently explored a number of sponsoring the analytical methods. To study nonlinear stage the stage developed a salt dome is the only numerical methods are used. Previous work on numerical analysis of nonlinear stage salt domes is limited with small areas[3-5]. Therefore not been carefully studied the impact of horizontal and vertical walls of field on growth and form hydrochloric diapir. In this work in response to the increasing power of personal computers are examined regularities of salt diapir in relatively large sized areas.

Problem statement

Initial-boundary value problem, describing the motion of non-uniform highly viscous incompressible fluid under gravity in flat production, is worded as follows: In the rectangular area Ω, the velocity $\vec{V} = (U, V)$, pressure ρ, density dynamic viscosity μ in time $t \in [0, T]$, satisfying the equations

$$A * \left(2 \frac{\partial}{\partial x} \left[\mu \frac{\partial U}{\partial x} \right] + \frac{\partial}{\partial y} \left[\mu \frac{\partial U}{\partial y} \right] + \frac{\partial}{\partial y} \left[\mu \frac{\partial V}{\partial x} \right] \right) - \frac{\partial P}{\partial x} = 0, \qquad \text{...(1)}$$

$$A * \left(2 \frac{\partial}{\partial y} \left[\mu \frac{\partial V}{\partial y} \right] + \frac{\partial}{\partial x} \left[\mu \frac{\partial V}{\partial x} \right] + \frac{\partial}{\partial x} \left[\mu \frac{\partial U}{\partial y} \right] \right) - \frac{\partial P}{\partial y} - \rho = 0, \qquad \text{...(2)}$$

$$\frac{\partial U}{\partial x} + \frac{\partial V}{\partial y} = 0, \qquad \text{...(3)}$$

$$\frac{\partial \rho}{\partial t} + U \frac{\partial \rho}{\partial x} + V \frac{\partial \rho}{\partial y} = 0, \qquad \text{...(4)}$$

$$\frac{\partial \mu}{\partial t} + U \frac{\partial \mu}{\partial x} + V \frac{\partial \mu}{\partial y} = 0, \qquad \text{...(5)}$$

Initial and boundary conditions on the border $\partial \Omega$

$$\rho(x,y,0) = \rho_0(x,y), \qquad 0 < \rho_2 \le \rho_0(x,y) \le \rho_1, \qquad \qquad \dots(6)$$

$$\mu(x,y,0) = \mu_0(x,y), \qquad 0 < \mu_2 \le \mu_0(x,y) \le \mu_1, \qquad \qquad \dots(7)$$

$$U\big|_{\partial\Omega\cdot[0,T]} = V\big|_{\partial\Omega\cdot[0,T]} = 0, \qquad \qquad \dots(8)$$

The system of Equations (1) to (5), initial and boundary conditions (6) through (8) written in dimensionless form. Here, *U, V*- respectively the horizontal and vertical components of velocity. The system of Equations (1) and (3) describes the motion of non-uniform highly viscous incompressible fluid in the gravity field, i.e. The Stokes equations and Equation (4), (5) take into account the conservation of density and viscosity at any point in time. Ratio is calculated by dividing the number of Froude Reynolds; $A = v_* \cdot U_* /(l_*^2 \cdot g)$ here g is the acceleration due to gravity, v_*, U_*, l_* – environment settings, respectively, kinematic viscosity and velocity and length field. In problems of gravitational instability there is no characteristic scale, speed, so as the last in a viscous speed $U_* = g^{\frac{1+n}{2}} L_*^{\frac{1+3n}{2}} v_*^{-n}$, where n – is an arbitrary number. Selecting the n in a certain way, we get the desired elevation speed of the model.

Numerical method of solution

For the numerical solution of systems of Equations (1) and (3) uses an iterative process based on the scheme of splitting physical processes[6]. Let the analyzed area Ω covered with uniform currents x and y grid cells:

$$\Omega = \begin{cases} x_{i+\frac{1}{2}} = i * h_x, & h_x > 0, \ i = 0,1,\dots\dots,M \\ y_{j+\frac{1}{2}} = j * h_y, & h_y > 0, \ j = 0,1,\dots\dots,N \end{cases}$$

Where h_x, h_y- the size of the grid, *M, N*- the number of steps the grid respectively in the directions of x-and y.

In the first phase of the scheme of splitting the implicit schema is a preliminary value velocity:

$$\frac{U^{n+\frac{1}{2}} - U^n}{\omega} = A \cdot \left[2 \cdot \left(\mu^m U_x^{n+\frac{1}{2}} \right)_x + \left(\mu^m U_y^{n+\frac{1}{2}} \right)_y + \left(\mu^m V_x^{n+\frac{1}{2}} \right)_y \right] - P_x^n \qquad \dots(9)$$

$$\frac{V^{n+\frac{1}{2}} - V^n}{\omega} = A \cdot \left[2 \cdot \left(\mu^m V_y^{n+\frac{1}{2}} \right)_y + \left(\mu^m V_x^{n+\frac{1}{2}} \right)_x + \left(\mu^m U_y^{n+\frac{1}{2}} \right)_x \right] - P_y^n, \qquad \ldots(10)$$

Equation (9) is in pixels $(i + \frac{1}{2}, j)$, , of the grid and equation (10)-in pixels $(i, j + \frac{1}{2})$.

For illustrative purposes, for example, $(\mu^m U_x^{n+\frac{1}{2}})_x$ a member of the sign points to $(i + \frac{1}{2}, j)$ read:

$$\left[\mu_{i+1, j}^m (U_{i+\frac{3}{2}, j}^{n+\frac{1}{2}} - U_{i+\frac{1}{2}, j}^{n+\frac{1}{2}}) - \mu_{i, j}^m (U_{i+\frac{1}{2}, j}^{n+\frac{1}{2}} - U_{i-\frac{1}{2}, j}^{n+\frac{1}{2}}) \right] \times \frac{1}{h_x^2}.$$

The superscript denotes m - a temporary equations and n - number of iterations to perform the loop.

In the second phase, searched the interim field speed, $\vec{V}^{n+\frac{1}{2}} = (U^{n+\frac{1}{2}}, V^{n+\frac{1}{2}})$ taking into account the conditions of the solenoid velocity is the pressure out $P_{i,j}^{n+1}$ of the equation:

$$P_{xx}^{n+1} + P_{yy}^{n+1} = \frac{1}{\omega} (U_x^{n+\frac{1}{2}} + V_y^{n+\frac{1}{2}}) + P_{xx}^n + P_{yy}^n. \qquad \ldots(11)$$

Equation (11) shall be calculated in points (i, j).

In the third stage, $\vec{V}^{n+1} = (U^{n+1}, V^{n+1})$ find out equations:

$$\frac{U^{n+1} - U^{n+\frac{1}{2}}}{\omega} = -(P_x^{n+1} - P_x^n), \qquad \ldots(12)$$

$$\frac{V^{n+1} - V^{n+\frac{1}{2}}}{\omega} = -(P_y^{n+1} - P_y^n) \qquad \ldots(13)$$

Equations (12) and (13) respectively in the same points that (9) and (10).

For the numerical solution of Eq. (4), (5) with initial conditions (6), (7) respectively, used conservative difference scheme against the flow of the step[7] at a time is selected, taking into account sustainability and the monotony schema:

$$\tau \leq \frac{h_x h_y}{h_x \underbrace{\max}_{\Omega}\left|U^{n+1}\right| + h_y, \underbrace{\max}_{\Omega}\left|V^{n+1}\right|} \qquad \dots(14)$$

For solving Equations (9)-(10) uses the top relaxation. According to calculations of the difference scheme (9) to (13) is absolutely stable. Parameter ω is selected, taking into account the rapid convergence of the iteration process.

So, the proposed algorithm for the numerical solution of tasks (1)-(8) is as follows: Let μ^m, ρ^n known (to $m = 0$ для μ и ρ this and will the initial data). Then unknown U^m, V^m, P^m is iterative process with the repetition of the above three steps in fulfilling the conditions

$$\max_{\Omega}\left(\left|U^{n+1} - U^n\right| + \left|V^{n+1} - V^n\right|\right) \leq \varepsilon \cdot \omega$$

Iterative process ends. This means that on m - -time step values are defined U^m, V^m, P^m. The explicit difference scheme is evaluated against the flow of the unknown in step ρ^{m+1}, μ^{m+1} at $(m + 1)$- a time. To find U^{m+1}, V^{m+1}, P^{m+1} again is an iterative process. Similarly, all values U^s, V^s, P^s, μ^s, ρ^s ($s = 0, 1, 2,....., L$) are defined up to a necessary t_L layer over time. Considered by the numerical method is suitable in all distributions, viscosity and density characteristic of sedimentary cover in natural conditions.

Analysis of the results of the calculation

Study for numerical instability of two-layer model of the array a saline environment where less dense layer is located below the denser (suprasalt species). The model is that each layer of homogeneous density and viscosity and various sectors can be of different power (height), density and viscosity. The number of the sections adapted from top to bottom. The properties of each layer are written with subscript indicating its number, for example, μ_2, ρ_2, h_2- viscosity, density and power of the second layer, i.e., salt.

If the boundary of the layer model, even for as long as there is a delicate balance. This is due to the fact that the horizontal component of the pressure gradient is zero. For dome-formation is necessary roughness on boundary layer section. Fig. 1-3 shows the evolution of boundary layers for three different models, differing from each other only by the area or the same thing-the horizontal and vertical size of the layers. The size of the area and time of development of gravitational instability are figures in the dimensionless form. Initial roughness on all models is a small cap at the border section of the layers.

From the figure, the primary salt dome is formed from the initial perturbations due to the outflow of the salt from the parent layer. The seam around the primary form of the dome deflections (compensatory trench), which later formed the secondary dome (Fig. 1). Due to the outflow of salt from a reservoir in the secondary dome, around them are secondary deflections. Later one of them is tertiary dome (Fig. 2). Depending on the horizontal size of a saline aquifer such domes in natural conditions may be several dozen.
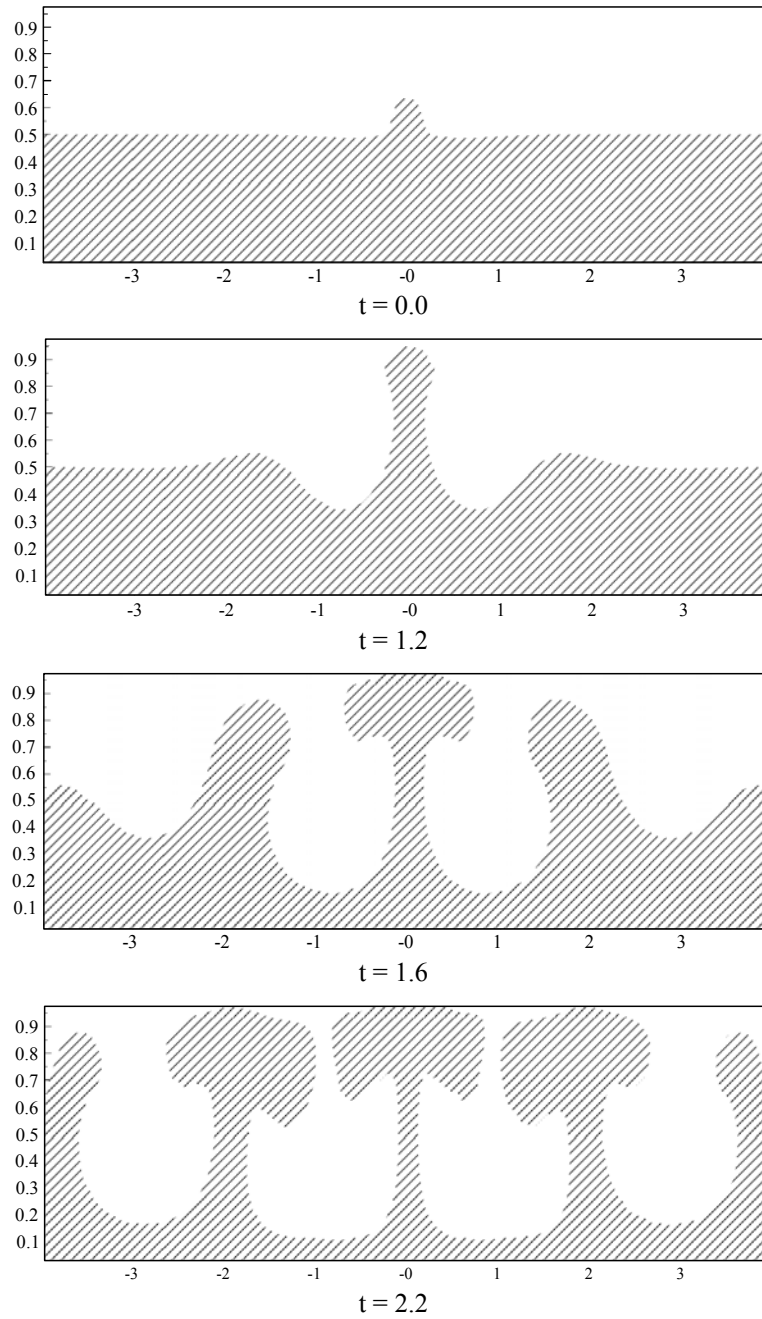
They all belong to the same OBD-engine, as their occurrence to primary dome. From a comparison of Fig. 1 and 2 shows that the secondary domes in Fig. 1 it is also influenced by the sagging and the proximity of vertical wall area, while the secondary dome in Fig. 2 are only because of sagging.

t = 0   t = 1.2

t = 1.6   t = 2.6
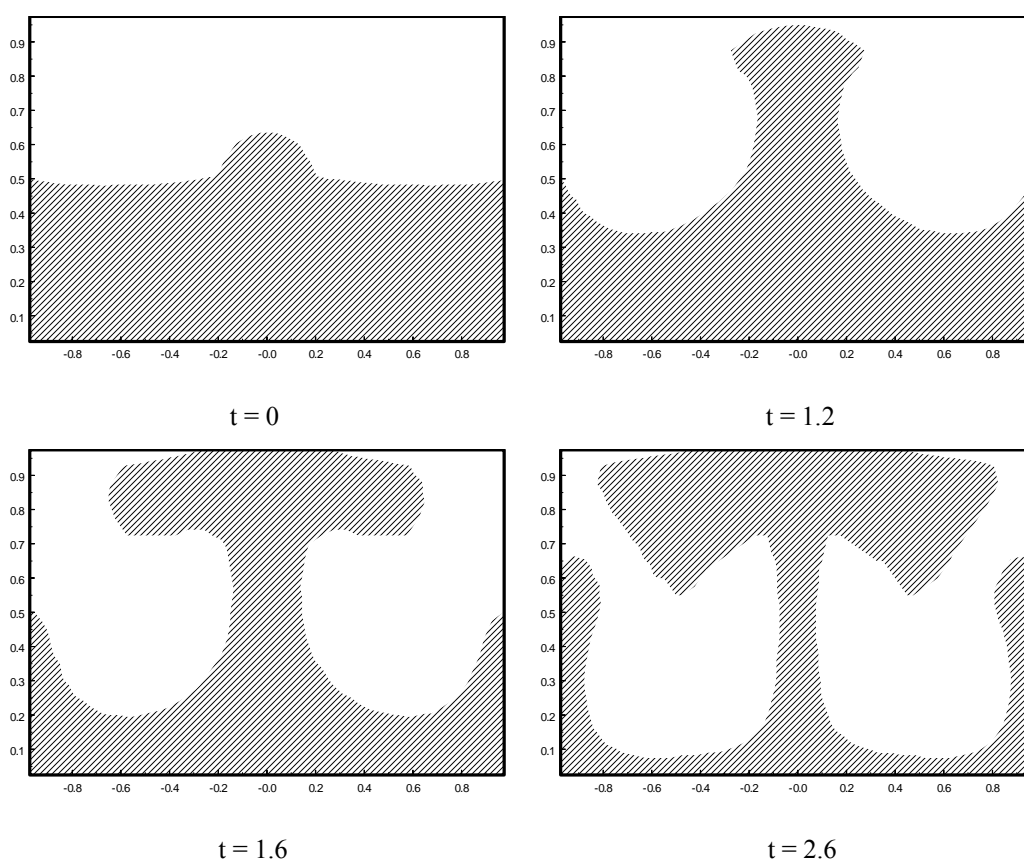
Fig. 1: Evolution of boundary layers in the process of gravitational instability.
The parameters of the model: $\mu_1 = 2{,}6 \cdot 10^{18}\, \kappa\varepsilon/(\text{м} \cdot c)$, $\rho_1 = 2{,}6 \cdot 10^3\, \kappa\varepsilon/\text{м}^3$ $h_1 = 4500\text{м}$;
$\mu_2 = 2{,}2 \cdot 10^{18}\, \kappa\varepsilon/(\text{м} \cdot c)$, $\rho_2 = 2{,}2 \cdot 10^3\, \kappa\varepsilon/\text{м}^3$ $h_2 = 4500\text{м}$.
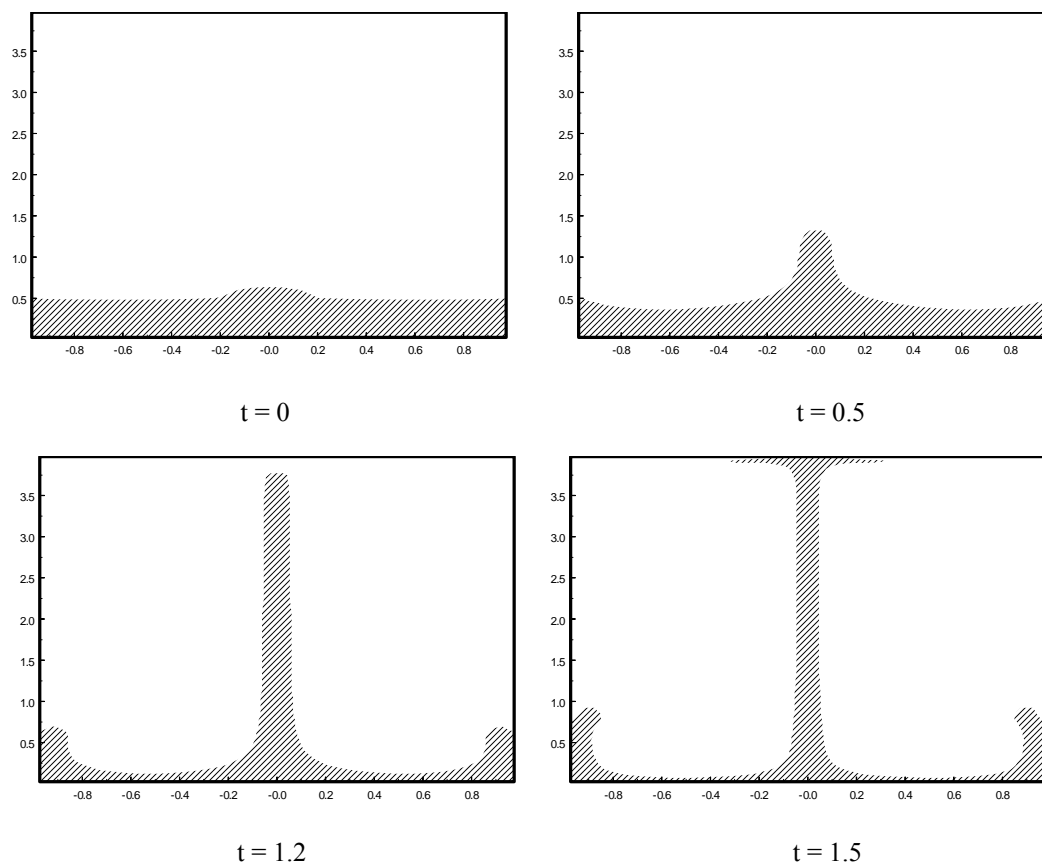
Fig. 2: Evolution of boundary layers in the process of gravitational instability.
The parameters of the model: $\mu_1 = 2{,}6 \cdot 10^{18} \, \kappa z/(\text{м·с})$, $\rho_1 = 2{,}6 \cdot 10^3 \, \kappa z/\text{м}^3$ $h_1 = 4500\text{м}$;
$\mu_2 = 2{,}2 \cdot 10^{18} \, \kappa z/(\text{м·с})$, $\rho_2 = 2{,}2 \cdot 10^3 \, \kappa z/\text{м}^3$ $h_2 = 4500\text{м}$.

In Fig. 1 and 3 presented the evolution of boundary layers for models that differ only in the capacity of suprasalt species or the same thing the distance between the dome and the top horizontal wall. From the figures it is clear that with increasing power suprasalt rock salt domes acquire a columnar shape, i.e., almost all the same width. Such domes are called diapir, i.e., the type of piercing the dome (Fig. 3). With approximately equal power sections of the upper part of the dome are growing, and the dome before reaching the upper wall is for mushroom head shape (Fig. 1).

t = 0

t = 0.5

t = 1.2

t = 1.5

Fig. 3: Evolution of boundary layers in the process of gravitational instability. The parameters of the model: $\mu_1 = 2{,}6 \cdot 10^{18}\ \kappa\varepsilon/(\text{м} \cdot c)$, $\rho_1 = 2{,}6 \cdot 10^3\ \kappa\varepsilon/\text{м}^3$ $h_1 = 18000\text{м}$; $\mu_2 = 2{,}2 \cdot 10^{18}\ \kappa\varepsilon/(\text{м} \cdot c)$, $\rho_2 = 2{,}2 \cdot 10^3\ \kappa\varepsilon/\text{м}^3$ $h_2 = 4500\text{м}$.

CONCLUSION

Comparison of flow patterns in three versions of calculations you can make the following conclusions: rising power of layers with constant horizontal size of the transverse

dimensions of the domes are increasing, the number of inactive domes, gravitational instability is faster. With the increase of the number of established sizes of horizontal domes is increased.

In the Caspian basin salt domes are the giants in its central part, where it was originally bedded salt of high power arrays. In the peripheral part of the Caspian Depression in relation to the small capacity of salt domes are small. Consequently, the obtained numerical results are correct and confirm the regularities of formation of salt-dome structures in the natural environment.

REFERENCES

1.   A. Yu and A. Kosygin, Fundamentals of Tectonics Oil Fields (1995) p. 511.

2.   H. Ramberg, The Force of Gravity and Deformation in the Crust. Per. from English, - M.: Nedra (1985) p. 400.

3.   W. D. Woid and H. J. Neugebauer, Finite Element Models of Density Instabilities by Means of Bicubic Spline Interpolation-Phys. Earth Planet. Inter., **21** (1980) pp. 176-180.

4.   S. Zaleski and P. Julien, Numerical Simulation of Rayleigh-Taylor Instability for Single and Multiple Salt Diapirs, Tectonophysics, **206** (1992) pp. 55-69.

5.   M. K. Orunkhanov and A. G. Tanirbergenov, Numerical Simulation of the Formation of Oil Salt Domes, Oil and Gas, **2** (2000) pp. 25-37.

6.   O. Belotserkovsky, Numerical Modeling in Continuum Mechanics, Moscow: Nauka (1984) p. 520.

7.   P. Roach, Computational Fluid Dynamics, Springer-Verlag (1980) p. 616.